Available online at www.sciencedirect.com
ScienceDirect
Optics Communications 270 (2007) 63–67
OPTICS COMMUNICATIONS
www.elsevier.com/locate/optcom

Transient temperature profile in the gain medium of CW- and end-pumped passively Q-switched microchip laser

Jianlang Li *, Jun Dong, Musha Mitsurua, Akira Shirakawa, Ken-ichi Ueda

Institute for Laser Science, University of Electro-communications, Tokyo 182-8585, Japan

Received 15 February 2006; received in revised form 29 June 2006; accepted 24 August 2006

Abstract

The transient temperature profile in CW- and end-pumped passively Q-switched (PQS) microchip laser is investigated qualitatively by treating the population inversion (thereby the thermal load) as the sawtooth function of the time. The numerical results reveal not only the dynamics of thermal buildup, but also the dependence of the quasi-steady-state temperature rise and the repetitively oscillatory amplitude on the incident pump power and the pulse repetition rate of PQS laser. The abruptly ascending branch of the repetitive temperature oscillation is synchronized with the pulsing stage of PQS laser. As the result, the abrupt temperature transition during the pulsing stage would introduce the fluctuation into the PQS pulse parameters (pulse energy, pulse width, and peak power) via temperature-dependent stimulated emission and thermal lensing effect.

Keywords: Passively Q-switched; Microchip laser; Transient temperature

1. Introduction

The CW- and end-pumped solid-state laser passively Q-switched (PQS) by an intracavity saturable absorber (SA) is a common technique used to generate the short pulses. A major problem of this technique is the large jitters in pulse parameters-width, repetition rate and peak power. The up to 20% variation in pulse amplitude and large perturbation in periodicity at higher pump powers have been reported in a end-pumped passively Q-switched Nd^{+}:YAG microchip laser [1]. This Q-switch instability also occurs systematically in passively mode-locked laser [2]. Until now there are few authors take insight into the physical nature of this fluctuation, partly because the pulse instability can be attributed fictitiously to the technical factors such as thermal and mechanical instability of the saturation absorber.

Our motivations to investigate the transient temperature profile in PQS laser crystal are based on the following two considerations. Firstly, the temperature variation of gain medium has significant effect on the lasing properties of the laser via temperature-dependent stimulated emission [3–10] or thermal lensing effect [11,12]. And secondly, due to the inversion buildup in the pumping cycle and the subsequent extraction in the pulsing stage, the population inversion of PQS microchip laser and then the thermal load exhibit the repetitively pulsed evolution. Therefore, it is essential to investigate the transient temperature profile induced by the time-dependent thermal load in PQS laser crystal and subsequent effects on the pulse parameters (pulse energy, pulse width and peak power).

The transient thermal profile in repetitively pumped laser rods previously has been described in Koechner's seminal work [13]. Nevertheless it is only applicable for the case that both periods of the pump pulse and the heat removal in the laser rod are far larger than the pump pulse width, and inapplicable for the case of the repetitive thermal load in PQS laser, in which the pulse-like width is comparable with its interval. In addition, the comprehensive description of the temperature profile induced by the repetitive thermal load need to solve the sets of partial differential equations (PDEs) consisting of the laser rate equations

* Corresponding author. Tel.: +81 424435708; fax: +81 424858960.
E-mail address: j-li@ils.uec.ac.jp (J. Li).

0030-4018/$ - see front matter © 2006 Elsevier B.V. All rights reserved.
doi:10.1016/j.optcom.2006.08.043

and thermal conductivity equation, which is quite complicated in mathematics. Due to this practical difficulty, how the temperature evolves in PQS laser crystal is not investigated until now.

In this paper, we take the example of CW- and end-pumped microchip PQS Yb:YAG laser PQS by a saturable absorber to numerical simulating the temperature variation in the gain medium. In Section 2, the thermal model in laser crystal with typical boundary condition is built, and the repetitive thermal load is treated as a sawtooth function of time and is compared with other numerical method. In Section 3, the parabolic heat equation is solved in Matlab PDE toolbox, the qualitative results on the transient temperature variation in PQS microchip laser crystal is given. In the last section, the results are summarized and the conclusions are given.

2. Theoretical model

The arrangement of the present thermal modelling is applicable for the CW- and longitudinally-pumped microchip laser crystal PQS by a saturable absorber. The periphery of microchip laser crystal is held at room temperature (300 K) by an actively cooled heat sink. Fig. 1 shows a side and end view of the microchip laser crystal and heat sink. The transient temperature distribution in cylindrically symmetrical microchip gain medium follows the partial differential equation

$$\frac{\rho C}{K_C}\frac{\partial T}{\partial t}-\frac{1}{r}\frac{\partial}{\partial r}\left(r\frac{\partial T}{\partial r}\right)+\frac{\partial^2 T}{\partial z^2}=\frac{Q(r,z,t)}{K_C}, \tag{1}$$

with the boundary conditions at the crystal surfaces are

$$T=300\ \mathrm{K},\quad \text{for } r=r_0$$
$$\frac{\partial T}{\partial z}=h(300-T),\quad \text{for } z=-l/2$$
$$\frac{\partial T}{\partial z}=-h(300-T),\quad \text{for } z=l/2. \tag{2a–c}$$

Here K_C is the thermal conductivity, ρ is the mass density, C is the specific heat of laser crystal, h is heat transfer coefficient between the laser crystal surface and air, T is the temperature as a function of time t, r_0 is the radius

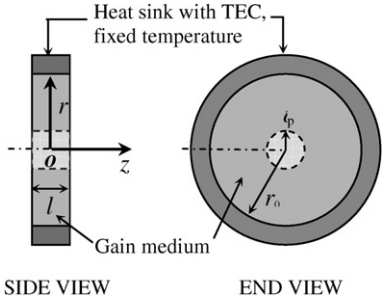

Fig. 1. Side view and end view of the microchip gain medium and thermoelectrically cooled (TEC) heat sink. The thickness and radius of the microchip gain medium is l and r_0, and the $1/e^2$ radius of the Gaussian pump beam is ϖ_p.

of microchip laser crystal, l is the crystal thickness, r and z are the radial and axial coordinates of the points in the microchip crystal respectively. To simplify the further investigation, the divergence of the pump beam in the thin laser crystal [11,12,14,15] is neglected, and the transversal distribution of the inversion is assumed to be uniform in the cylindrical-shaped pump area. The top-hat distributed thermal source density Q in the laser crystal due to incident pump power P_{in} can be given by [16]

$$Q(r,z,t)=\frac{\xi P_{in}}{\pi\omega_P^2}\sigma_{abs}[N_t-n(t)]\exp\left\{-\sigma_{abs}[N_t-n(t)]z-\left(\frac{r}{\omega_P}\right)^2\right\}, \tag{3}$$

where N_t is the total doping concentration of active ions in laser crystal, n is its inversion population density, σ_{abs} is the absorption cross section at pump wavelength, ξ is fractional thermal load, ϖ_P is the $1/e^2$ radius of the Gaussian pump beam.

The inversion population density n of the gain medium is accumulated nearly linearly in pumping cycle, and is dumped out rapidly during Q-switching. We approximately treat n as a sawtooth function of time t with the period $1/f$ (f, the repetition rate of Q-switched pulse), which has the following expression:

$$n(t)\approx(n_i+n_f)/2+(n_i-n_f)/2\cdot\mathrm{sawtooth}(2\pi\cdot f\cdot t). \tag{4}$$

Here n_i and n_f are the initial and final population inversion density of gain medium respectively [17], and sawtooth ($2\pi ft$) is the sawtooth function with a period of $1/f$. To verify this approximation intuitively, firstly we numerically solve the rate equations of the CW- and end-pumped passively Q-switched Yb:YAG/Cr^{4+}:YAG laser by applying Runga–Kutta method as described in [18], and plot the typical time evolution of the intra-cavity photon number density and the inversion population density in Fig. 2(a)

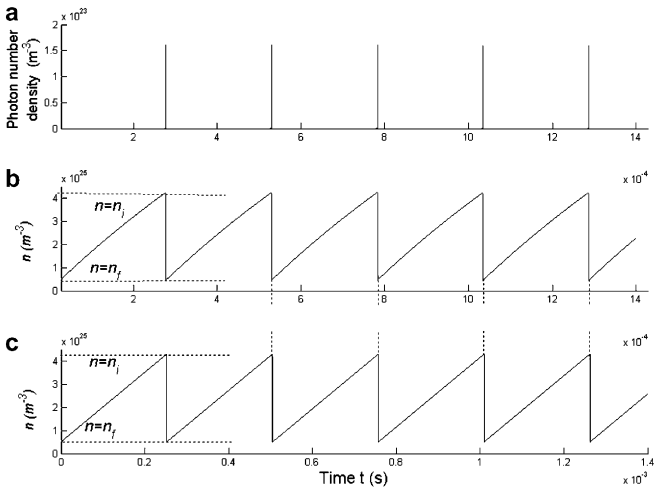

Fig. 2. The typical time evolution of the intra-cavity photon number density (a) and the inversion population density (b) in CW-pumped PQS laser. For comparing with (b), (c) presents is the time evolution of the inversion population density under the sawtooth function approximation as given in Eq. (4).

and (b). After substituting n_i, n_f and f derived from Fig. 2(b) into Eq. (4), the time evolution of the inversion population density under the sawtooth function approximation is plotted in Fig. 2(c). After comparing Fig. 2(c) with Fig. 2(b), it could be concluded the approximation to n in Eq. (4) can reproduces time evolution of n as well as Fig. 2(b). The sawtooth evolution of the inversion density can be better described analytically than that in Degnan paper [17], in particular for the slow increase of inversion density and determination of the repetition rate.

Therefore, after substituting Eq. (4) into Eq. (3), the time-dependent thermal load $Q(t)$ in PQS microchip laser, could be written out clearly in the form of the sawtooth function. If assuming n_i, n_f, f and P_{in} are known, it become possible to directly investigate the transient temperature distribution of the laser crystal by numerical solving Eq. (1) in the environment of the Matlab partial differential equation (PDE) toolbox.

In the following section we still take the example of the CW- and end-pumped passively Q-switched Yb:YAG/Cr^{4+}:YAG laser. The physical parameters of PQS Yb:YAG microchip laser are as follows, $\sigma_{abs} = 0.75 \times 10^{-20}\ cm^2$ at 940 nm, $\xi = 0.1$, $K_C = 14\ W\ m^{-1}\ K^{-1}$, $C = 0.59\ J\ g^{-1}\ K^{-1}$, $\rho = 4.56\ g\ m^{-3}$ and $h = 4\ W/m^2\ K$, $N_t = 3 \times 10^{20}\ cm^{-3}$, $n_i = 1 \times 10^{20}\ cm^{-3}$, $n_f = 5.69 \times 10^{19}\ cm^{-3}$. The pump beam $1/e^2$ radius $\varpi_p = 200\ \mu m$. The microchip Yb:YAG crystal radius $r_0 = 1$ mm and the thickness $l = 1$ mm. The radial and axial thermal time constants of the microchip laser crystal, are defined as [19]

$$\tau_r = \frac{C\rho}{K_C} r_0^2 \quad \text{and} \quad \tau_z = \frac{C\rho}{K_C} l^2, \tag{5a–b}$$

are $\tau_r = \tau_z = 190$ ms, respectively. The period $(1/f)$ of the Q-switched pulses, where f is usually in the range of ~kHz, is very short compared to the heat removal time τ_r and τ_z. After substituting these known parameters into Eqs. (3) and (4), and solving parabolic Eq. (1) with the pulsation source term and the boundary conditions Eq. (2) in the Matalb PDEtool environment, we could obtain the transient temperature variation of all the points inside the laser crystal when the time t varies.

3. Numerical results

The temperature variation induced by the thermal load in end-pumped PQS microchip laser is radially symmetrical. The thermal problem expressed in Eq. (1) can be treated as in 2-D geometry (r and z) when solving it in Matlab PDE toolbox. During our simulation, the time step is 50 ns, and the refined spatial mesh consists of 10821 nodes and 21312 triangles for the whole laser crystal.

The transient temperature variations as the function of time t at point A ($z = -0.45$ mm, $r = 0$) and B ($z = -0.45$ mm, $r = 0.1$) under different repetition rates f of PQS laser pulse are given in Fig. 3. Fig. 3(a) shows, when $f = 2$ kHz and $P_{in} = 5$ W, it take several tens of milliseconds for the temperature at points A and B to reach a

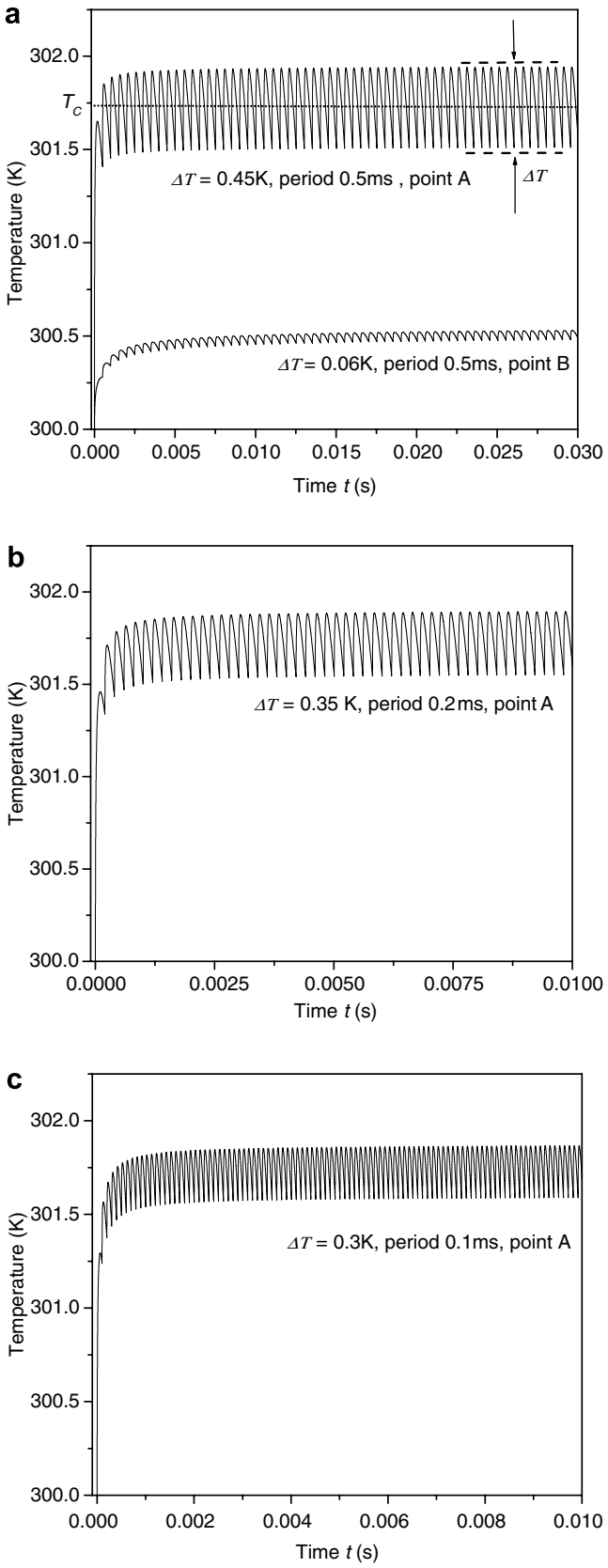

Fig. 3. The transient temperature variation of Yb:YAG crystal in end-pumped PQS laser when the incident pump power is 5 W and the PQS pulse repetition rates f varies. (a) $f = 2$ kHz, at point A and point B; (b) $f = 5$ kHz, at point A and (c) $f = 10$ kHz, at point A. For point A, the coordinates $r = 0$ mm, $z = -0.45$ mm; for point B, $r = 0.1$ mm, $z = -0.45$ mm.

quasi-steady-state. The quasi-steady-state temperature rise at point A of Yb:YAG microchip is $T_C = 301.7$ K with the repetitively oscillatory amplitude $\Delta T = 0.45$ K and the period 0.5 ms. Fig. 3(b) shows, when $f = 5$ kHz and $P_{in} = 5$ W, the transient temperature variation has $T_C = 301.7$ K, $\Delta T = 0.35$ K and 0.2 ms period. The case of $f = 10$ kHz and $P_{in} = 5$ W is given in Fig. 3(c), the transient temperature variation has $T_C = 301.7$ K, $\Delta T = 0.3$ K and 0.1 ms period. The periods of this repetitive temperature oscillation shown Fig. 3(a–c) are the same as the respective periods of the Q-switched laser pulse.

Fig. 4 plots the time correspondence between the time evolutions of n and the transient temperature at points A and B when $f = 2$ kHz and $P_{in} = 5$ W.

It is seen that from Figs. 3 and 4, when incident pump power P_{in} is fixed at a certain value, the temperature rise inside the PQS laser crystal reaches the quasi-steady-state in several tens milliseconds and remains the oscillatory behaviour; the period of this repetitive oscillation is the same as $1/f$. In addition, the pulsing stage of PQS laser [20,21] is synchronized with the abruptly ascending branches of the repetitive temperature oscillations at points A and B, while the pumping cycle just corresponds with the descending branches of the repetitive temperature oscillations.

Fig. 5 plots the transient quasi-steady temperature distribution profile inside the laser crystal at $t = 30$ ms when $f = 5$ kHz and $P_{in} = 10$ W. It shows that the thermal load in end-pumped PQS microchip laser only brings the large temperature rise in the central region where the pump light is present. As the pump area in the laser crystal is small (200 μm radius), thus only the small-volume central area of the radial direction has large temperature rise and fluctuation. And both temperature rise and repetitively oscillatory temperature amplitude decreases rapidly with the radius r. As a result, both T_c and ΔT at point B are much smaller than that ones at point A.

Fig. 6 plots the quasi-steady-state temperature rise T_C and the repetitively oscillatory amplitude ΔT at point A as the functions of PQS pulse repetition rate f when $P_{in} = 5$ W. It is seen that, when P_{in} is unchanged the temperature rise T_C at quasi-steady-state almost remains the same despite of f, and the oscillatory temperature amplitude ΔT is inversely proportional to f.

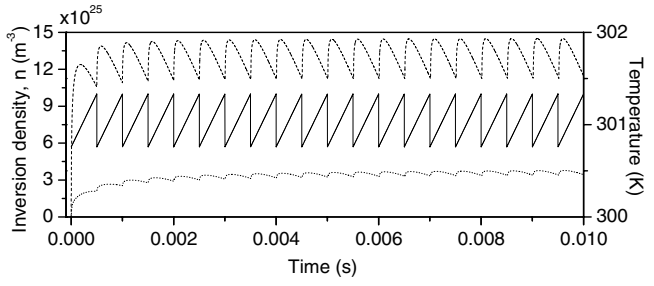

Fig. 4. The correspondence between the time evolutions of n and the transient temperature at points A and B when $f = 2$ kHz and $P_{in} = 5$ W. The dashed line represents the temperature variation at point A, and b the dotted line represents the temperature variation at point B, while the solid line plots the population inversion density inside the laser crystal.

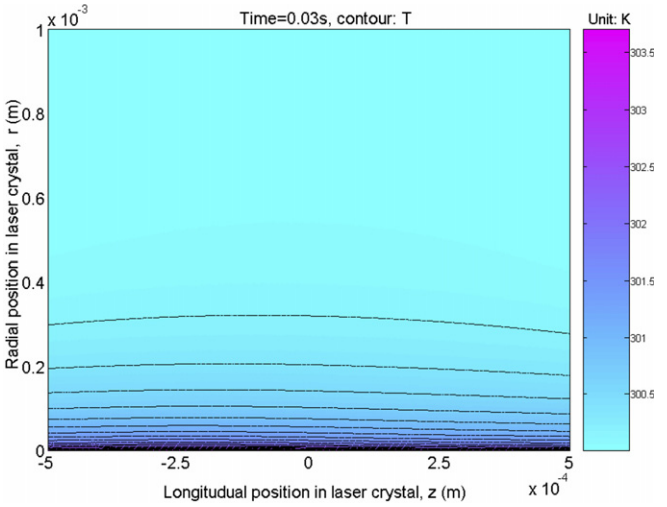

Fig. 5. The 20-level contour plot of the temperature distribution in laser crystal at $t = 0.03$ s when $P_{in} = 10$ W, $f = 5$ kHz.

Fig. 7(a) and (b) show T_C and ΔT at point A as the functions of the incident pump power P_{in} when $f = 5$ kHz, respectively. Obviously both T_C and ΔT are proportional to P_{in} when f is fixed at certain value.

The simulations above give the transient temperature variations at specified time and spatial steps, the mean temperature rise T_C is relatively small compared with the other experimental or theoretical data of Yb:YAG as given in [11]. Worthwhile to point out, T_C, ΔT and the time to reach the quasi-steady-state are dependent on how much of the time step and refined spatial mesh triangles are taken. When a smaller time step or much more refined spatial mesh triangles are applied, T_C, as well as ΔT and the time to reach the quasi-steady-state, becomes much larger and certainly close to the practical temperature variation in laser crystal, despite of the time-consuming calculation and requirement of big computer memory capacity when

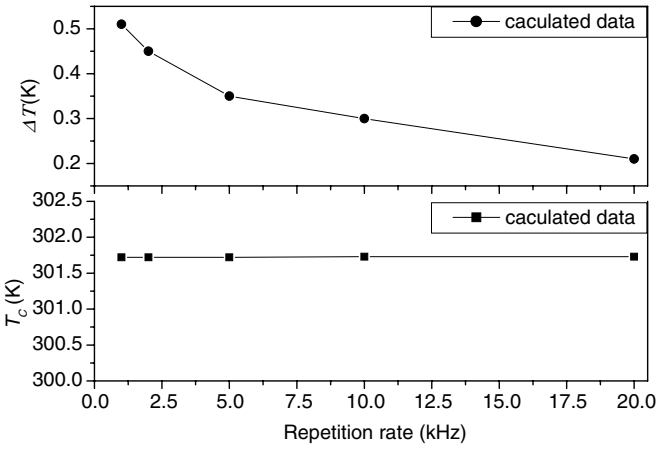

Fig. 6. The quasi-steady-state temperature rise T_C and the repetitively modulated amplitude ΔT at point A as the function of PQS pulse repetition rate f when $P_{in} = 5$ W.

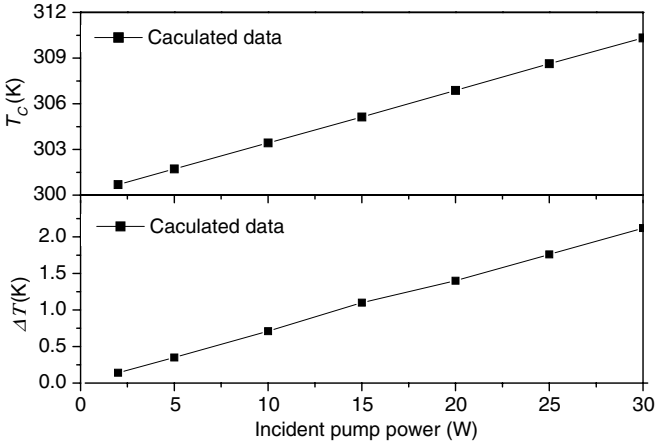

Fig. 7. The quasi-steady-state temperature rise T_C and the repetitively oscillatory amplitude ΔT as the function of the incident pump power when $f = 5$ kHz, respectively.

using Matlab PDE tools. Therefore, based on the practical difficulty encountered by us, we prefer to treat the numerical results above at specified temporal and spatial steps as the qualitative (/relative) ones rather than the quantitive (/absolute) ones.

4. Discussions and conclusions

Here we summarize the qualitative results obtained as follows:

For any given pump incident power above the threshold of PQS laser, the radially symmetrical temperature distribution reaches the quasi-steady state in several tens millisecond and remains the oscillatory behaviour. The buildup time of the quasi-steady-state temperature is comparable with the radial and axial thermal time constants of the microchip laser crystal. And the period of this repetitively oscillatory temperature is the same as the period ($1/f$) of PQS laser pulse, and the abruptly ascending branch of this repetitive oscillation is synchronized with the pulsing stage of PQS laser, while the descending branch of it just corresponds the pumping cycle of PQS laser at any point inside the laser crystal.

In addition, when the incident pump power is fixed, the repetitively oscillatory amplitude ΔT is inversely proportional to f, whereas the quasi-steady-state temperature rise T_C remains the same while f varies; when the repetition rate of Q-switched laser pulse is fixed, both T_C and ΔT are proportional to the incident pump power; i.e. $T_C \propto P_{in}$ and $\Delta T \propto P_{in}$.

In conclusion, the transient temperature profile in CW- and end-pump PQS microchip laser is investigated qualitatively by treating the population inversion (thereby the thermal load) as the sawtooth function of the time. The results reveal not only the dynamics of thermal buildup, but also the dependence of the quasi-steady-state temperature rise and the repetitively oscillatory amplitude on the incident pump power and the pulse repetition rate of PQS laser. As the result, the abrupt temperature transition during the pulsing stage could introduce the fluctuation into the PQS pulse parameters (pulse energy, pulse width, and peak power) by transient thermal lensing effect and/or temperature-dependent stimulated emission.

Being a simple approach, our model does not consider the effect of P_{in} on n_i, n_f and f and other factors such as pump divergence and inversion nonuniformity [11]. In practical microchip PQS laser, n_i, n_f and f are the functions of P_{in}, the M square factor of a pump beam could be in the range of 30–45 [11]. And also our model cannot cover the specific feedback of the transient temperature variation on the lasing properties of PQS laser. The comprehensive model that describes the interaction between the transient temperature and PQS laser parameters, requires to solve numerically the coupling between the PQS lasers rate equations and heat equation in both the temporal and spatial domains. In this case, Matlab PDE tools become inapplicable any more. The endeavour of seeking another mathematical method to carry out the simulation of the full problem (heat equation + PQS laser equations) is in progress.

References

[1] J.J. Zayhowski, C. Dill III, Opt. Lett. 19 (1994) 1427.
[2] N. Joly, S. Bielawski, Opt. Lett. 62 (2001) 692.
[3] C. Erlandson, G.F. Albrecht, S.E. Stokowski, J. Opt. Soc. Am. B 9 (1992) 214.
[4] J. Dong, M. Bass, Y. Mao, P. Deng, F. Gan, J. Opt. Soc. Am. B 20 (2003) 1975.
[5] S. Zhao, A. Rapaport, J. Dong, B. Chen, et al., Opt. Mat. 27 (2005) 1329.
[6] D.J. Ripin, J.R. Ochoa, R.L. Aggarwal, T.Y. Fan, Opt. Lett. 29 (2004) 2154.
[7] D.C. Brown, IEEE J. Sel. Topics Quantum Elect. 11 (2005) 587.
[8] T.Y. Fan, T. Crow, B. Hoden, Cooled Yb:YAG for high-power solid-state lasers, Proc. SPIE 3381 (1998) 200.
[9] T. Kasamatsu, H. Sekita, Y. Kuwano, Appl. Opt. 38 (1999) 5149.
[10] J. Kawanaka, K. Yamakawa, H. Nishioka, K.-i. Ueda, Opt. Express 10 (2002) 455.
[11] S. Chenais, F. Balembois, F. Druon, G. Lucas-Leclin, P. Georges, IEEE J. Quantum Elect. 40 (2004) 1217.
[12] S. Chenais, F. Balembois, F. Druon, G. Lucas-Leclin, P. Georges, IEEE J. Quantum Elect. 40 (2004) 1235.
[13] W. Koechner, J. Appl. Phys. 44 (1973) 3163.
[14] X. Zhang, A. Brenier, Q. Wang, Z. Wang, J. Chang, P. Li, S. Zhang, S. Ding, S. Li, Opt. Express 13 (2005) 7708.
[15] T. Taira, J. Saikawa, T. Kobayashi, R.L. Byer, IEEE J. Sel. Top. Quantum Elect. 3 (1997) 100.
[16] Y.F. Chen, T.M. Huang, C.F. Kao, C.L. Wang, S.C. Wang, IEEE J. Quantum Elect. 33 (1997) 1424.
[17] J.J. Degnan, IEEE J. Quantum Elect. 25 (1989) 214.
[18] J. Dong, Opt. Commun. 226 (2003) 337.
[19] U.O. Farrukh, A.M. Buoncristiani, C.E. Byvik, IEEE J. Quantum Elect. 24 (1988) 2253.
[20] T. Erneux, J. Opt. Soc. Am. B 5 (1988) 1063.
[21] T. Erneux, P. Peterson, A. Gavrielides, Eur. Phys. J. D 10 (2000) 423.